

Modeling of kink-shaped carbon-nanotube Schottky diode with gate bias modulation

Toshishige Yamada^{a)}

NASA Ames Research Center, M/S 229-1, Moffett Field, California 94035-1000

(Received 16 July 2001; accepted for publication 27 March 2002)

A model is proposed for the recent gate voltage V_G modulation experiment of a kink-shaped carbon nanotube (NT) Schottky diode [Z. Yao, H. Postma, L. Balents, and C. Dekker, *Nature (London)* **402**, 273 (1999)]. Since larger V_G increases both the forward and the reverse turn-on voltages of the diode, we show that: (1) the rectification must occur at the kink where the metallic and the semiconducting NTs meet, and not at the electrode contact, and (2) the semiconducting NT must be n type. The turn-on voltages are derived analytically as a function of V_G considering the electrode contact contribution and a good agreement is obtained with the experimental data. © 2002 American Institute of Physics. [DOI: 10.1063/1.1481213]

Recently, the Delft group has observed rectifying current–voltage characteristics for a fused kink-shaped carbon nanotube (NT) metal–semiconductor (MS) diode.¹ They applied the gate voltage V_G to change the carrier density in the semiconducting NT and modulated the diode characteristics. Previous analysis focused on the two-terminal properties with a one-dimensional (1D) coherent transport model in a self-consistent field.² In this letter, we will emphasize the three-terminal properties, i.e., how V_G modulates the diode characteristics. From this V_G dependence, we show that: (1) the rectification occurred at the NT MS junction and not at the electrode contact, and (2) the carriers involved in the transport must be electrons rather than holes, unlike commonly observed p -type NTs.

In Ref. 1, they placed NTs on TiAu electrodes on a SiO_2 /doped-Si substrate (backgate) as in Fig. 1(a) and applied V_G to the backgate with electrode 3 grounded under a low temperature environment of 100 K. The circuit between electrodes 0 and 1 showed linear characteristics (110 k Ω) without noticeable V_G dependence. Thus, the left NT was metallic. However, the circuit between electrodes 1 and 3 across 2 showed rectifying characteristics with appreciable V_G dependence as in Fig. 1(b). Therefore, the right NT had to be semiconducting. We introduce an equivalent circuit with drain current I_D and voltage V_D at electrode 1. A linear resistor R_1 represents contact 1. V_G modulates the carrier density in the semiconducting NT and a capacitor C_{NT} represents the capacitance with respect to the substrate. The metallic and the semiconducting NTs meet at kink 2, and a MS junction J_2 is formed. The semiconducting NT reaches electrode 3 and a semiconductor–metal (SM) junction J_3 is formed. For rectification to take place, either J_2 or J_3 should be a Schottky diode and the other should be a resistive element. In fact, if both are Schottky diodes, then J_2 and J_3 are either front-to-front ($-|>|-|<|-$) or back-to-back ($-|<|-|>|-$) connected by sharing the semiconducting NT and will allow only negligible current through them. If both are resistive

elements allowing current in both polarities, then there is no mechanism for rectification.

The forward direction occurred when $V_D > 0$.¹ Thus, two equivalent circuits are possible: J_2 is a Schottky diode with an n -type NT and J_3 is a resistor as in Fig. 2(a), or J_2 is a resistor and J_3 is a Schottky diode with a p -type NT as in Fig. 2(b). We introduce forward and reverse turn-on voltages for a diode, V_{onF} and V_{onR} , respectively,³ corresponding to the onset of I_D . The experimental V_G dependence is such that: if $V_G < V'_G$, then $0 < V_{onF} < V'_{onF}$ and $V_{onR} < V'_{onR} < 0$ as in Fig. 1(b), where a prime indicates a quantity at V'_G . Or increasing V_G shifts both V_{onF} and V_{onR} in the positive V_D direction.

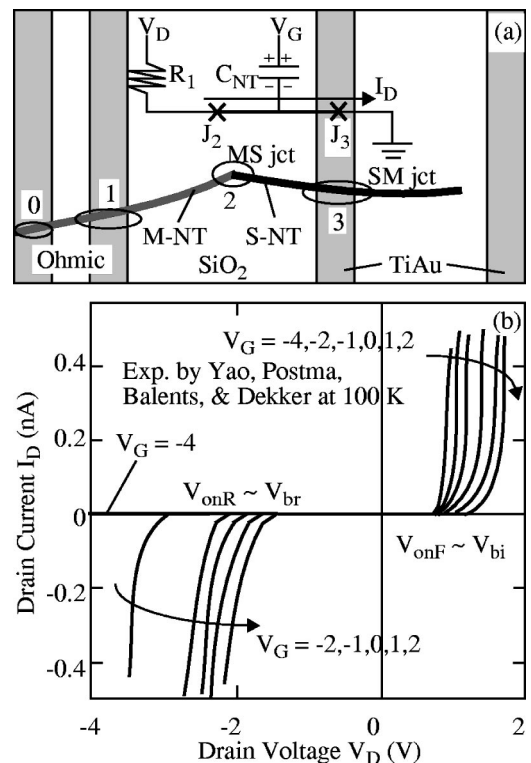


FIG. 1. (a) Experimental setup and its equivalent circuit; (b) I_D – V_D characteristics between electrodes 1 and 3 with V_G as a parameter at 100 K (experiment by Yao *et al.*, Ref. 1).

^{a)}Electronic mail: yamada@nas.nasa.gov

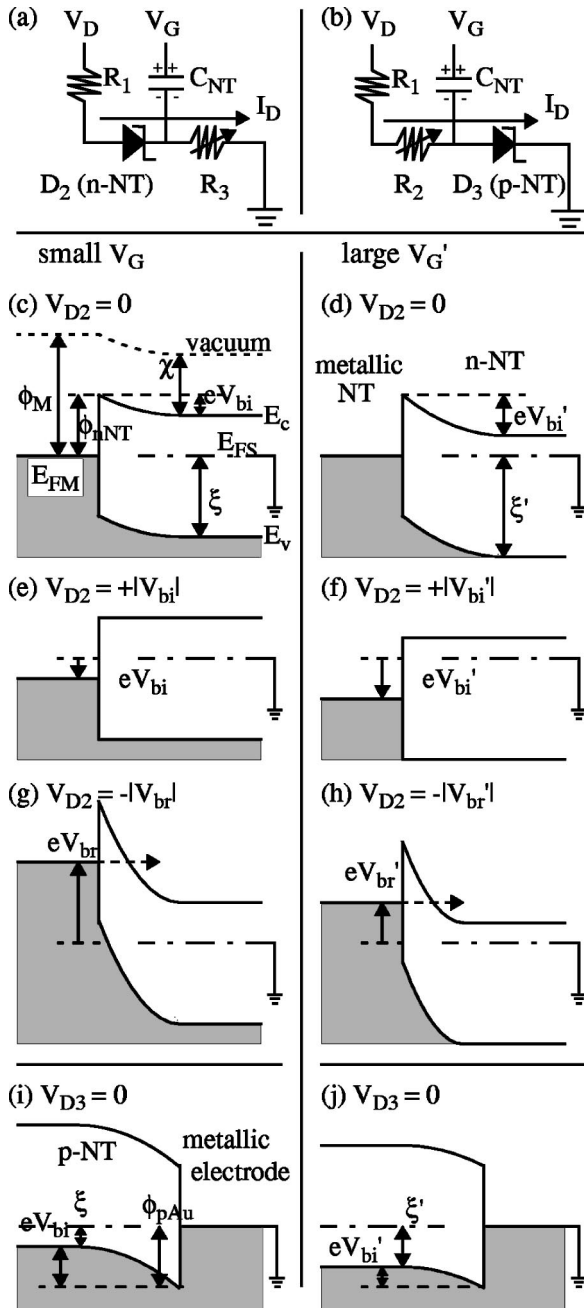


FIG. 2. Rectification mechanisms: (a) equivalent circuit with a fused NT MS junction D_2 of n type and an ohmic contact R_3 with a capacitor C_{NT} ; (b) equivalent circuit with an ohmic contact R_2 and an NT-electrode SM junction D_3 of p type; (c)–(h) energy band diagrams for selected V_{D2} s in the n -NT scenario of (a); (i)–(j) energy band diagrams for $V_{D3} = 0$ in the p -NT scenario of (b). Small V_G (left) and large V'_G (right) cases are examined, where ϕ_M is a work function, ϕ_{nNT} and ϕ_{pAu} are Schottky barriers, E_{FM} and E_{FS} are electrochemical potentials, ξ is a chemical potential, E_c and E_v are conduction and valence band edges with a band gap E_g , V_{bi} and V_{br} are built-in and breakdown voltages, and χ is an electron affinity.

Such V_G dependence is possible with an n -NT, but not with a p -NT. The band diagrams for Schottky diode D_2 of n type in Fig. 2(a) are shown in Figs. 2(c)–2(h) for selected D_2 voltages V_{D2} s, and those for D_3 of p type in Fig. 2(b) are shown in Figs. 2(i)–2(j) for null D_3 voltage V_{D3} , respectively. We compare small V_G (left) and large V'_G (right) cases. ϕ_M is a metallic NT work function. ϕ_{nNT} and ϕ_{pAu} are Schottky barriers for electrons at D_2 and holes at D_3 , respectively. E_{FM} and E_{FS} are electrochemical potentials (Fermi levels) in the metallic and the semiconducting NTs.

E_c and E_v are conduction and valence band edges with a band gap E_g . ξ is a chemical potential $E_{FS} - E_v$ and χ is an electron affinity. V_{bi} (>0) is a built-in voltage and V_{br} (<0) is a breakdown voltage. e (>0) is the unit charge.

We examine the n -NT scenario with D_2 as in Fig. 2(a) and compare the influences of V_G . Increasing V_G results in higher electron density, and ξ increases. Thus, $\xi < \xi'$ and we may think that the doping is effectively increased. Since ϕ_{nNT} is independent of V_G , $V_{bi} < V'_{bi}$ as shown in Figs. 2(c) and 2(d). In the thermionic emission³ (Ref. 2 estimated a thick Schottky barrier of several nanometers), the forward turn-on occurs when $V_D \sim V_{bi}$. Therefore, $V_{onF} < V'_{onF}$, as in Figs. 2(e) and 2(f). This is consistent with the experiment. The reverse turn on occurs when the gradient and the width of the Schottky barrier exceed certain thresholds or $V_D \sim V_{br} = -|V_{br}|$. This is the beginning of the tunneling breakdown. The effective doping is larger for larger V_G , leading to the thinner Schottky barrier as in Figs. 2(g) and 2(h). Thus, $-|V_{br}| < -|V'_{br}|$ and $V_{onR} < V'_{onR}$. This is also consistent with the experiment.

However, neither trends for V_{onF} and V_{onR} are explained by the p -NT scenario with D_3 as in Fig. 2(b). Increasing V_G results in lower hole density and ξ increases. Thus, again $\xi < \xi'$. However, $V_{bi} > V'_{bi}$ for holes as shown in Figs. 2(i) and 2(j). Thus, $V_{onF} > V'_{onF}$ in the forward direction, but this is contrary to the experiment. In the reverse direction, the effective doping is smaller for larger V_G and the Schottky barrier is thicker. Thus, $-|V_{br}| > -|V'_{br}|$ and $V_{onR} > V'_{onR}$. This is again contrary to the experiment. Therefore, we conclude that: (1) the rectification occurred at D_2 , and (2) the NT must be n type.

We will express V_{onF} and V_{onR} as a function of V_G based on this view. Since the onset of I_D is our present interest, we do not solve the transport problem but identify the diode turn-on voltages. This is practically enough for many electronics applications.^{3,4} V_G attracts or repels electrons through contact 3 (electrodes are infinite charge reservoirs), and causes a linear change in ξ , such that $\xi(V_G) = \xi(0) + \alpha e V_G$. The coefficient α is related to the NT state density and C_{NT} ,⁵ and thus depends on the quasi-1D NT band structure as well as the detailed device geometry including the SiO_2 layer. The NT specific information is embedded in α . By inspecting the band diagram in Fig. 2(c), we have $e V_{bi} = \phi_{nNT} - [E_g - \xi(V_G)]$. The forward turn on is achieved by applying $V_{D2} = V_{bi}$. Thus, the forward turn-on modulation by V_G is given by $\Delta V_{bi}(V_G) = \alpha \Delta V_G$.

The reverse turn on for a different V_G occurs when the Schottky barrier has the same slope (electric field) at the junction. In this case, transport electrons see the same Schottky barrier height and the width since ϕ_{nNT} is independent of V_G . The electric field at the junction is proportional to $[(V_{bi} + |V_{br}|)N_d^+]^{1/2}$ based on the planar junction theory.³ By equating $(V_{bi} + |V_{br}|)N_d^+$ for finite and zero V_G cases with an ionized donor density N_d^+ , we have $(V_{bi0} + |V_{br}| - \alpha V_G)(N_{d0}^+ + N_{d0}^+ V_G / \beta) = (V_{bi0} + |V_{br0}|)N_{d0}^+$, where the subscript 0 refers to $V_G = 0$. $V_G = -\beta$ (<0) is a voltage such that the electrons are repelled completely, and the NT becomes intrinsic. The reverse turn on is achieved by applying $V_{D2} = V_{br}$. Therefore, the modulation is given by $\Delta V_{br}(V_G) = -(|V_{br}| - |V_{br0}|) = \alpha \Delta V_G - \Delta[(V_{bi0} + |V_{br0}|) /$

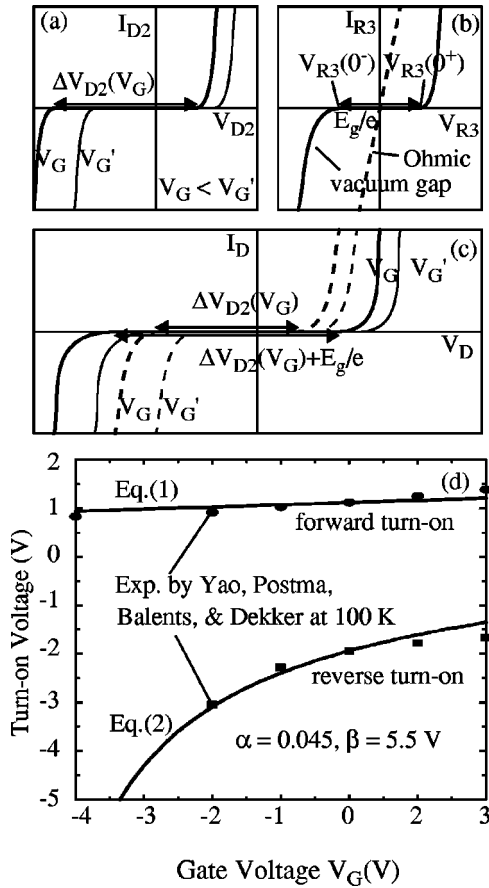


FIG. 3. Comparison to experiment: (a) schematic $I_{D2}-V_{D2}$ characteristics for Schottky diode D_2 with two gate biases V_G (thick line) $< V_G'$ (thin line); (b) schematic $I_{R3}-V_{R3}$ characteristics for Schottky contact R_3 with vacuum-gap (solid line) and ohmic (dotted line) modes; (c) schematic I_D-V_D characteristics for the entire circuit with two gate biases and two contact modes; (d) comparison of Eqs. (1) and (2) to experimental $V_{onF}(V_G)$ (circles) and $V_{onR}(V_G)$ (squares) at 100 K.

$(1 + V_G/\beta)$. The term αV_G appears in both ΔV_{bi} and ΔV_{br} since it represents the same effect of V_G upon ξ .

Practically, V_{D2} cannot be directly measured due to the electrode contacts. In Ref. 1, R_1 was about a half of 110 k Ω and can be safely neglected, but R_3 cannot be. Figures 3(a) and 3(b) show current–voltage characteristics $I_{D2}-V_{D2}$ for D_2 and $I_{R3}-V_{R3}$ for R_3 , respectively. Then, $I_D = I_{D2} = I_{R3}$ and $V_D = V_{D2} + V_{R3}(I_D)$ appear finally as in Fig. 3(c). If R_3 is ohmic (dotted line), $V_{R3}(0^+) = V_{R3}(0^-) = 0$ and the final I_D -absent domain remains the same, ΔV_{D2} . However, if R_3 has the “vacuum-gap”⁶ characteristics (solid line), V_{onF} and V_{onR} are offset by $V_{R3}(0^+)$ and $V_{R3}(0^-)$, respectively, where $V_{R3}(0^+) - V_{R3}(0^-) = E_g/e$. Thus, the final I_D -absent domain is $\Delta V_{D2} + E_g/e$. Since the experimental $V_{onF} = 0.8-1.4$ V¹ was somewhat beyond the theoretical $E_g/e = 1.2$ V for (7,1)/(8,0) kink-shaped MS NT,⁷ we assume the “vacuum-gap” mode for R_3 . In fact, the I_D -absent domain is pronounced at lower temperatures⁸ and this is consistent with the measurement at 100 K.¹ The turn-on voltage modulation by V_G including the R_3 contribution is given by

$$V_{onF}(V_G) = V_{onF}(0) + \alpha V_G, \quad (1)$$

$$V_{onR}(V_G) = V_{onR}(0) + \alpha V_G + (V_{onF}(0) + |V_{onR}(0)| - E_g/e) V_G / (\beta + V_G), \quad (2)$$

where the partition of E_g/e for $V_{onF}(0)$ and $|V_{onR}(0)|$ does not have to be known. Equations (1) and (2) are now ready for experimental comparison. They will be extended for other gated MS diode analysis, with an appropriate inclusion of the contact contributions.

We have chosen $\alpha = 0.045$ and fitted Eq. (1) to the experimental $V_{onF}(V_G)$.¹ With a choice of $\beta = 5.5$ V (compatible with the negligible reverse I_D at $V_G = -4.0$ V),¹ Eq. (2) recovers the experimental $V_{onR}(V_G)$ quite well as in Fig. 3(d), and this gives the foundation for our modeling. Quasi-1D junction field⁹ and image potential³ effects would not be relevant and are not included in our model, but they could be necessary in the analysis for finite I_D .

Although the present NT must be n type, NTs have been p type in many cases.¹⁰ Several mechanisms have been proposed for this p -type behavior, and oxidation in air is one of them. The thermoelectric experiments showed that NTs are originally n type due to unintentional doping in the production process, but turn to p type after the air oxidation.^{11,12} The oxidation typically occurs on the order of hours at 300 K with the binding energy of the adsorbed oxygen ~ 5000 K.¹² Thus, at 100 K, the oxidation is significantly suppressed ($e^{-5000/100}/e^{-5000/300} \sim 3 \times 10^{-15}$), and this could be a possible mechanism for the n type here. The trapped charges in or on the SiO_2 layer³ might have contributed to the n -type behavior. The apparent difference of the present fused MS NT compared to the previous all semiconducting NTs may also be relevant.

In summary, Delft’s gated NT MS diode measurements are studied. It is shown that the rectification occurred at the kink of the NT junction and the NT must be n type. We have derived turn-on voltages V_{onF} and V_{onR} as a function of V_G analytically, and recovered the experimental data well.

The author acknowledges fruitful discussions with C. W. Bauschlicher, Jr., T. R. Govindan, and M. Meyyappan.

¹Z. Yao, H. W. Ch. Postma, L. Balents, and C. Dekker, *Nature (London)* **402**, 273 (1999).

²A. A. Odintsov, *Phys. Rev. Lett.* **85**, 150 (2000).

³S. M. Sze, *Physics of Semiconductor Devices*, 2nd ed. (Wiley, New York, 1981); Y. Uemura and M. Kikuchi, *Semiconductors—Theory and Applications* (Shokabo, Tokyo, 1978) [in Japanese].

⁴This is similar to the role of a turn-on voltage 0.7 V for a typical Si $p-n$ junction diode.

⁵ V_G induces charges $-C_{NT}V_G$ in the NT, and this is converted to $\Delta\xi$. Thus, $\alpha \sim C_{NT}/[C_{NT} + e^2D(\xi_0)]$, where $D(\xi_0)$ is a NT state density at $V_G = 0$.

⁶T. Yamada, *Appl. Phys. Lett.* **78**, 1739 (2001).

⁷L. Chico, V. H. Crespi, L. X. Benedict, S. G. Louie, and M. L. Cohen, *Phys. Rev. Lett.* **76**, 971 (1996).

⁸H. R. Shea, R. Martel, T. Hertel, T. Schmidt, and Ph. Avouris, *Microelectron. Eng.* **46**, 101 (1999); C. Zhou, J. Kong, and H. Dai, *Appl. Phys. Lett.* **76**, 1597 (2000).

⁹F. Leonard and J. Tersoff, *Phys. Rev. Lett.* **84**, 4693 (2000).

¹⁰S. J. Tans, A. R. M. Verschueren, and C. Dekker, *Nature (London)* **393**, 49 (1998); R. Martel, T. Schmidt, H. R. Shea, T. Hertel, and Ph. Avouris, *Appl. Phys. Lett.* **73**, 2447 (1998); T. Yamada, *ibid.* **76**, 628 (2000).

¹¹G. U. Sumanasekera, C. K. W. Adu, S. Fang, and P. C. Eklund, *Phys. Rev. Lett.* **85**, 1096 (2000).

¹²K. Bradley, S.-H. Jhi, P. G. Collins, J. Hone, M. L. Cohen, S. G. Louie, and A. Zettl, *Phys. Rev. Lett.* **85**, 4361 (2000).